

# Study on surface subsidence law in mining area based on SBAS-InSAR technology

Guangchun Liu

Liaoning Institute of Science and Technology, Benxi, Liaoning, 117004, China

**Abstract:** In view of the problems of traditional mine monitoring technology, which is time-consuming, laborious, small amount of monitoring data, and affected by weather, this paper selects radar satellite earth observation technology, adopts SBAS-InSAR image processing method, obtains the surface settlement changes in the study area, and analyzes several typical settlement funnels in the mining area: the data results show that the maximum settlement in the Fengyuan Village mining area is more than -30mm, and the maximum settlement in the Loess Temple mining area and Shagou mining area is more than -50mm. The Kentielinggou mining area and the Heishiyuan mining area have the fastest settlement at two points, with a maximum settlement of more than -90mm.

**Keywords:** Shendong mining area; SBAS-InSAR technology; Sentinel-1 imagery; Mine settlement monitoring; Characteristic analysis.

## 1. Introduction

China has very rich mineral resources, coal mining in the contribution to the country's economic and social development at the same time, coal mining activities caused by the surface deformation seriously damaged land resources and ecological environment. Therefore, it is very important to monitor the settlement of the mine safely. The traditional monitoring method has many defects, such as long detection time, high economic consumption, short storage time of monitoring points, and poor adaptability to the external environment. In contrast, Synthetic Aperture Radar Interferometry (InSAR) has the advantages of low cost, high efficiency, and low external environment. Among them, the most commonly used InSAR treatment method is the Small Base Line Subset (SBAS) InSAR technology, which can continuously monitor the study area and has the ability to monitor a large area of small deformations for a long time.

In our country, researchers have used InSAR technology to monitor subsidence in mining areas for a relatively short time, but the research in this field has made rapid progress and achieved many phased results. In 2021, Yang et al. processed the Sentinel-1 data obtained from 2014 to 2015 by differential interferometry, and compared the settlement distribution images in the two years, and found that the interference images obtained by D-InSAR showed the same law as the actual settlement curve in the study area. This study shows that the D-InSAR technology can effectively grasp the law of land subsidence [1]. In 2022, Wang et al. obtained the surface deformation information before and after the recent goaf in Shandong mining area, used D-InSAR and SBAS-InSAR to process the SAR images of the mining area, and analyzed the ability of these two technologies to monitor the surface deformation, providing a new reference method for the early warning of mine earthquakes in the mining area [2]. In order to improve the accuracy of InSAR deformation monitoring and expand the application scope of this technology, Zhang Tongkang et al. [3] proposed a SBAS-InSAR-based mining subsidence monitoring based on 44 Sentinel-1A data from October 2018 to March 2020 to Mengcun Coal Mine in Binchang Mining Area, Shaanxi Province, and obtained the

annual average settlement rate and time series cumulative settlement value of the mining area. In 2019, Dong Shaochun et al. used SBAS-InSAR technology and 36 Sentinel-1A SAR images collected in 2015~2018 to extract the land deformation rate of Changzhou City, and the results showed that the land subsidence in Wujin District was increasing and expanding over time [4]. In 2022, Luo Xuewei et al. proposed a PS-based SBAS-InSAR method, which uses the stable PS points obtained by the PS-InSAR method as the ground control points in SBAS-InSAR orbital refining, so as to improve the accuracy of the deformation monitoring results, and the effectiveness of the method is verified by a ground collapse as an example [5]. InSAR technology was first used to observe a wide range of deformation fields on the earth's surface, such as the movement measurement of glaciers and the displacement measurement of earthquakes, but with the development of science and technology, the application of this technology has been continuously improved, and the ability to process data has also been continuously improved, and InSAR technology has also been gradually applied to the subsidence monitoring of oil, coal, metal mining areas and other ground subsidence monitoring. InSAR technology has achieved remarkable results in monitoring mining deformation in mining areas, and different deformation monitoring methods have their own advantages and disadvantages. Researchers at home and abroad have carried out relevant research on the comparison, combination or integration of various InSAR technologies to monitor and analyze the deformation of mining areas. In 2018, Depin Ou et al. fused DInSAR and pixel shift tracking methods to monitor coal mine surface deformation [6]. In 2019, Kamila Pawluszek-Filipiak et al. proposed the integration of DInSAR and SBAS technologies to take advantage of the advantages of both methods and overcome the disadvantages of both methods, to monitor the complete deformation of the study area, which can effectively monitor mining-related settlement [7]. In the same year, Govil used multi-view Sentinel 1 images and D-InSAR technology to obtain the deformation of the Korba Chhattisgarh coalfield in India, which helped prevent the occurrence of geological disasters such as land subsidence [8]. In 2021, Bassols Joan Botey et al. obtained D-InSAR data

by persistent scatterer interferometry processing of Sentinel-1A data, and conducted experiments on the processed data according to the existing hydrogeological conditions, and analyzed the spatial distribution and temporal evolution of surface deformation, which showed that the D-InSAR observations are crucial in identifying the process of ground deformation and its diffusion range [9].

## 2. InSAR principle

### 2.1. Principles of InSAR

As a cutting-edge space geodetic method, synthetic aperture radar interferometry (SAR) is based on the use of two beams of coherent light from different light sources to irradiate a specific object at the same time, and researchers can calculate the true distance of the object according to the phase difference generated by the two rays. In the signal acquisition process of SAR technology, the radar antenna first emits a specially crafted radar wave in the direction of the satellite. These waves are reflected back after touching objects on the ground, forming an echo. Subsequently, the antennas on the satellite capture these echoes in a time series and immediately record their intensity. Varying intensities of the echo will show different levels of brightness on the SAR image. Therefore, radar interferometry mainly focuses on analyzing the phase relationship between the echo signals received by two antennas at different locations on the ground at the same location.

The antenna positions of satellite S1 and satellite S2 show obvious differences at different times, R1 and R2 represent the distance between the antennas of the two satellites to the target point O respectively, and the distance between the two satellite antennas, that is, the baseline length is represented by B, the angle between the baseline and the horizontal direction is denoted as  $\alpha$ , the vertical height of the satellite antenna from the ground is H represented in the figure, the angle formed between the direction of the satellite line of sight and the vertical direction is denoted as  $\theta$ , and the wavelength of the signal transmitted by the radar is expressed as  $\lambda$ .

The phase of the observed target point O at S1 in Figure 1:

$$\phi_1 = -\frac{2\pi}{\lambda} \cdot 2R_1 = -\frac{4\pi}{\lambda} \cdot R_1 \quad (1)$$

The phase of the observed target point O at S2 in Figure 1:

$$\phi_2 = -\frac{2\pi}{\lambda} \cdot 2R_2 = -\frac{4\pi}{\lambda} \cdot R_2 \quad (2)$$

The phase difference between points S1 and S2 is:

$$\Delta\phi = \phi_1 - \phi_2 = \frac{4\pi}{\lambda} \cdot \delta R \quad (3)$$

Since R1 is much larger than the baseline length B and the distance difference  $\delta R$ , the equation can be simplified:

$$\theta = \alpha - \arcsin \frac{\lambda \Delta\phi}{4\pi B} \quad (4)$$

The elevation h is calculated:

$$h = H - R_1 \cos \theta \quad (5)$$

From the results obtained from the above calculation method, it can be seen that if the exact values of 1 and 2,  $\lambda$ ,  $\alpha$ ,

H, and B can be obtained, the value of elevation h can be obtained, and the surface elevation of the target area can also be calculated accordingly.

### 2.2. SBAS-InSAR technology

Berardino, Lanari et al. have proposed short baseline set differential interferometry (SBAS-InSAR), which focuses on low-resolution and large-scale time series landmark deformation monitoring. The key to this technology is to set a specific threshold for spatiotemporal baselines, filter out radar images that meet the conditions for interferometric pairing, and then construct a series of data sets. The cumulative deformation data of surface points is accurately calculated by using the least squares method to solve the deformation of each data set, and finally the singular value decomposition (SVD) technology is used to integrate the information of different datasets.

## 3. Engineering application examples

### 3.1. Overview of the study area

Shendong Mining Area Shendong Mining Area is the abbreviation of Shenfu Dongsheng Mining Area. It is now the largest underground coal mining site in China, as shown in Figure 1. The study area is located at 39.1°~39.4°N, 111.2°~110.5°E, in the north of Yulin City, Shaanxi Province, extending to the south of Ordos City, Inner Mongolia Autonomous Region, and the adjacent part of Baode County, Shanxi Province, forming a unique geographical junction. At the same time, it is also located on the southern border of the Mu Us Desert, the fifth largest desert in China, and the Loess Plateau, which is famous for its drought and lack of rainfall and serious soil erosion.

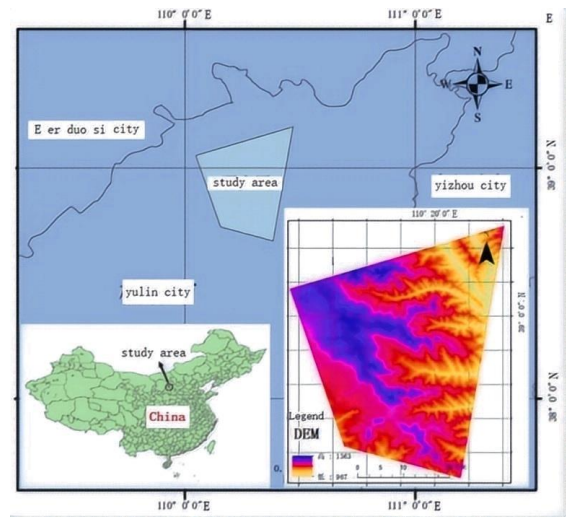


Fig. 1 Geographical location and topographic status of the study area

### 3.2. Data

#### 3.2.1. Sentinel-1 SAR data

The image data used in this SBAS-InSAR experiment is Sentinel-1A satellite imagery, the data are all from the <https://search.asf.alaska.edu> website, a total of 28 satellite data, these data types are single view complex data (SLC), the beam mode is IW mode, the polarization mode is VV ascending satellite data, time coverage: from September 25, 2016 to August 27, 2017, During this period, the revisit frequency of the satellite is once every 12 or 24 days, and the specific data and parameters are shown in Table 1 below.

**Table 1.** Sentinel Image Observation Time List

NO.	time	NO.	time	NO.	time	NO.	time
1	20160925	8	20161218	15	20170312	22	20170604
2	20161007	9	20161230	16	20170324	23	20170628
3	20161019	10	20170111	17	20170405	24	20170710
4	20161031	11	20170112	18	20170417	25	20170722
5	20161112	12	20170204	19	20170429	26	20170803
6	20161124	13	20170216	20	20170511	27	20170825
7	20161206	14	20170228	21	20170523	28	20170827

**3.2.2. DEM Data**

Download the \_NASA data of Shaanxi Province at \_DEM\_30m resolution and crop the range required for the study, as shown in Figure 1. The DEM is mainly to provide a reference for the undulating changes of the surface topography in the mining area, so as to eliminate the influence of topography on the surface subsidence.

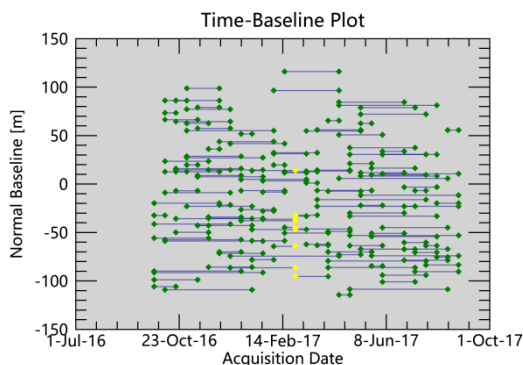
**3.2.3. Precise ephemeris data**

There are three main types of orbital data from Sentinel-1 satellites: bulid-in orbits, POD Restituted Orbit, and POD Precise Orbit Ephemerides. Among them, buile-in orbits is the orbit information that comes with the data itself, and the accuracy is the worst. PODRestituted Orbit (POD regression orbit data) is a relatively accurate orbit data, and the positioning accuracy is better than 10cm; POD Precise Orbit Ephemeris is the most accurate orbit data, with a positioning accuracy of better than 5cm. A total of 28 documents were downloaded from September 25, 2016 to August 27, 2017, using precision orbit data from [https://s1qc.asf.alaska.edu/aux\\_poeorb/](https://s1qc.asf.alaska.edu/aux_poeorb/) website.

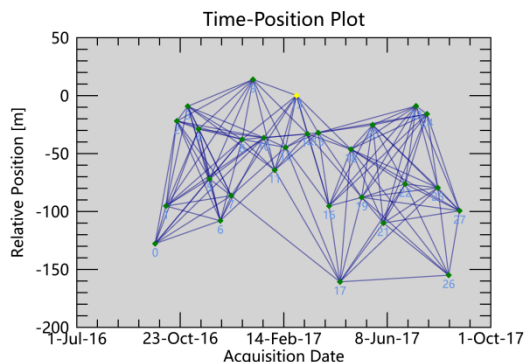
**3.3. Result analysis**

(1) Spatial baseline distribution

In this experiment, the SARScap data processing tool in ENVI software was used to obtain the Sentry 1 radar image data, and the spatiotemporal baseline distribution map was obtained, as shown in Figure 2. The spatial baseline quality is to ensure the distribution relationship of satellites in time and space during surface monitoring in the study area, and the yellow dot in the connection map is the super main image, and the green dot is the image. Through the analysis of the output results, the maximum time baseline and the maximum space baseline meet the requirements.



(a) Baseline distribution over time



(b) Spatial baseline distribution map

**Fig. 2** Distribution of spatiotemporal baselines

(2) Analysis of surface subsidence process in the study area

In ENVI, the radar data processing results are analyzed for spatiotemporal comparison, as shown in Figure 3. Over time, some subsidence funnels have gradually appeared on the surface, and the maximum subsidence has exceeded 110mm. Some of these areas have shown an uplift trend, and the uplift area is mainly distributed in the northern part of the study area, and it is found that there are open-pit mine dumps and an aluminum ore dump in the north.

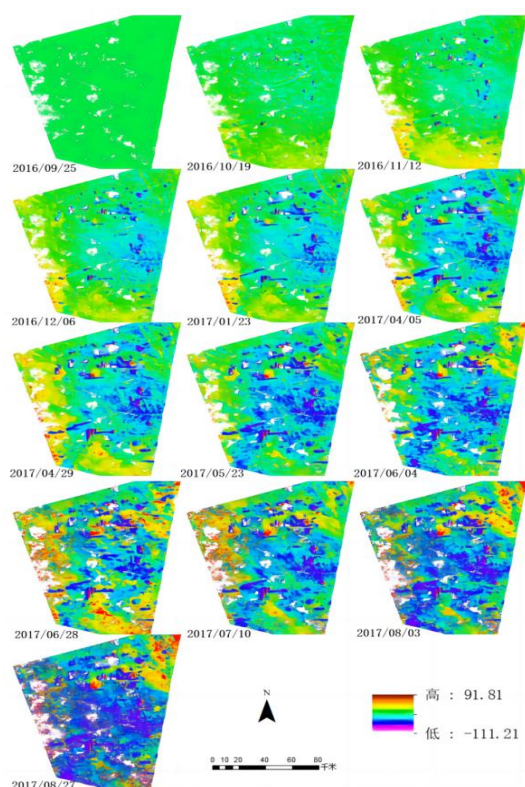


**Fig. 3** Spatiotemporal subsidence process of subsidence in the study area

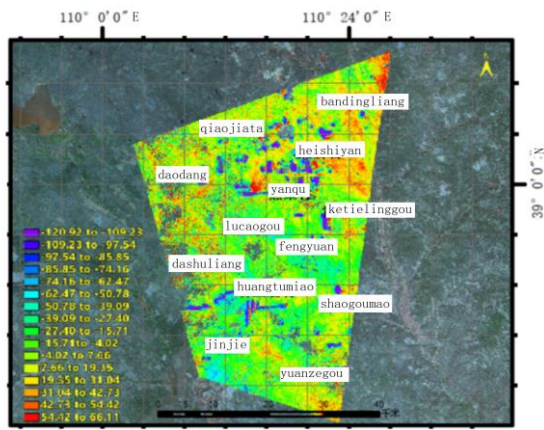


Fig. 4 Spatial distribution and characteristics of subsidence area

According to the analysis of Figure 5, A, B, C, D and E all showed a downward trend throughout the year, and there was no excessive fluctuation during this period, among which the settlement of point A was relatively gentle, with a maximum settlement of -32.6mm, and the settlement rate of points B and D was faster than that of point A, with the maximum

settlement of -55.91mm and -68.4mm respectively, and the settlement rate of C and E was the fastest. The maximum sedimentation reaches -95.11 mm and -92.3 mm, respectively.

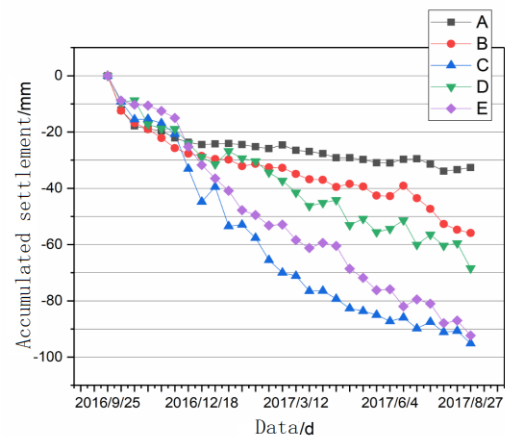


Fig. 5 Cross-sectional view of the mining area of Huangtumiao Village

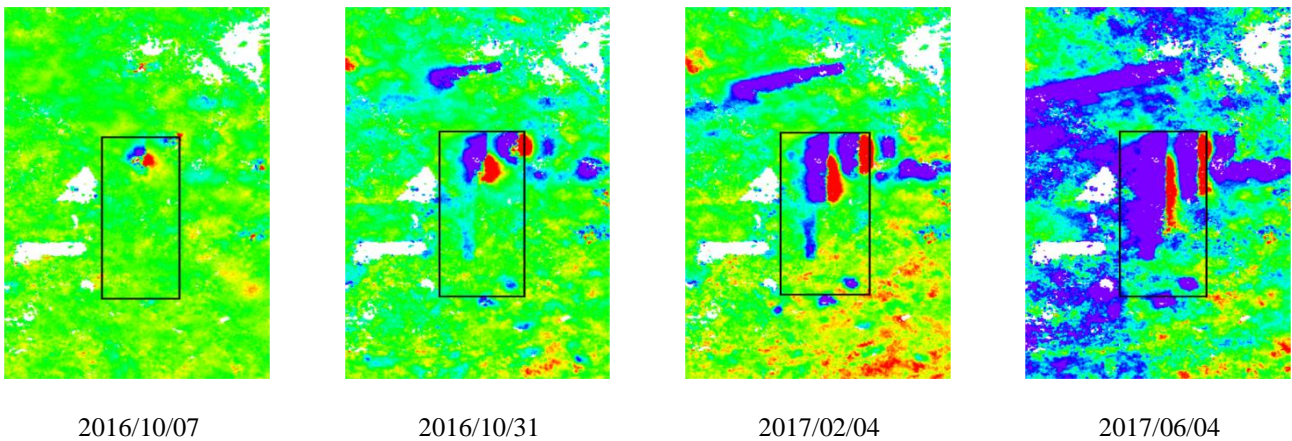


Fig. 6 The settlement process of the 5025-working face in the Loess Temple mining area

As shown in Figure 5, it is observed that there is an obvious settlement funnel in the Loess Temple mining area, and the settlement funnel extends around the center of the settlement funnel and gradually distributes in a strip pattern. The subsidence range gradually extends from north to south along the working face, and there is basically no settlement at first. With the advancement of mining progress, the amount of subsidence gradually increases, and the phenomenon of land subsidence appears, and its amplitude increases with time until it reaches a relatively stable state. This process clearly demonstrates the close link between mining activities and surface subsidence. Through the monitoring of the subsidence area of the mining area, we found that the formation of the subsidence basin is extremely consistent with the actual working face 5025 mining in the mining area. This consistency is not only reflected in the spatial distribution, but also in the change of time series, which provides strong evidence for the study of geological changes in mining areas. With the gradual increase of land subsidence in the mining area of the coal mining face, a large number of coal mines have been mined, resulting in large-scale land subsidence. As the mining intensity increases, the subsidence range spreads outward around the center of the subsidence funnel. For the deformation monitoring of this mining area, the maximum cumulative settlement monitored by SBAS-InSAR is -

56.71mm.

## 4. Conclusion

The use of satellite remote sensing technology can be very effective in monitoring the surface subsidence of the mining area, the monitoring efficiency is much higher than the traditional measurement method, and the satellite monitoring can penetrate the clouds, not limited by climate and weather conditions, it has a better integration with the environment remote sensing is easier to achieve. However, this method still has some drawbacks, such as incoherence and large deformation, while small deformation can be fully monitored, which can provide monitoring data support for mine safety production and mine safety.

## Acknowledgment

This paper has received support from the Doctoral Initiation Fund of Liaoning Province for the research on mining subsidence monitoring based on long-term InSAR technology (2407B13). This thesis was supported by the Liaoning Provincial Service Local Fund and the Geological Hazard Sensitivity Monitoring, Early Warning, and Disaster Mechanism Research in Dandong City (LJKFZ20220282).

## References

- [1] Yang Jie, Zeng Qiang. Analysis of surface subsidence by D-InSAR technology in Shuixigou fire area[J]. Mining Safety and Environmental Protection, 2021, 48 (03): 68-73.
- [2] Wang Fengyun, Tao Qiuxiang, Chen Yang, et al. Coal Mine Safety, 2022, 53(06): 195-203.
- [3] Zhang Tongkang. Research on mining subsidence monitoring and dynamic prediction based on SBAS-InSAR[D]. Xi'an University of Science and Technology, 2021.
- [4] Dong Shaochun, Chong Yahui, Hu Huan, et al. Land subsidence monitoring in Changzhou city from 2015 to 2018 based on time-series InSAR[J]. Journal of Nanjing University(Natural Science), 2019, 55(03): 370-380.
- [5] Luo Xuewei, Xiang Xiqiong, Lv Yadong. PS correction for inSAR deformation monitoring of a collapse time series in Longli[J]. Remote Sensing of Natural Resources, 2022, 34(03): 82-87.
- [6] Ou D, Tan K ,Du Q , et al. Decision Fusion of D-InSAR and Pixel Offset Tracking for Coal Mining Deformation Monitoring[J]. Remote Sensing, 2018, 10(7): 1055-1055.
- [7] Pawluszek-Filipiak K, Borkowski A .Integration of DInSAR and SBAS Techniques to Determine Mining-Related Deformations Using Sentinel-1 Data: The Case Study of Rydułtowy Mine in Poland[J]. Remote Sensing, 2020, 12(2): 242-242.
- [8] Monika, H. G ,Subhanil G .Underground mine deformation monitoring using Synthetic Aperture Radar technique: A case study of Rajgamar coal mine of Korba Chhattisgarh, India[J]. Journal of Applied Geophysics, 2023, 209.
- [9] I B J B, Enric S V, Michele C, et al. D-InSAR monitoring of ground deformation related to the dewatering of construction sites. A case study of Glòries Square, Barcelona[J]. Engineering Geology, 2021, 286 (prepublish) :106041.